Pergamon

Int. J. Solids Structures Vol. 31, No. 24, pp. 3419–3442, 1994

0020-7683/94 $7.00 + .00

0020-7683(94)00072-7

ELASTIC BEAM ON A RIGID FRICTIONAL FOUNDATION UNDER MONOTONIC AND CYCLIC LOADING

S. STUPKIEWICZ and Z. MRÓZ
Institute of Fundamental Technological Research, Warsaw, Poland

(*Received* 17 *January* 1994; *in revised form* 23 *April* 1994)

Abstract—An elastic beam resting on a frictional foundation and loaded by the concentrated force or moment applied at its tip is considered. The evolution of slip zones along the beam is discussed for both monotonic and cyclic loading. It is shown that an infinite number of slip zones develop and their propagation satisfies in some cases a self-similarity property. Transient hysteretic effects under cyclic loading are discussed. The closed form analytical solution is presented for the elastic friction model in the case of monotonic loading.

1. INTRODUCTION

The interaction of an elastic body with the frictional foundation under monotonic or varying loads involves progressive development of slip zones in the contact area and for some classes of problems also variation of this area with varying normal traction. Two examples of such slip evolution were discussed by Jarzębowski and Mróz (1994), namely the case of a tensile strip resting on the foundation obeying Coulomb friction rule and relative slip or sliding of two spheres under normal and tangential forces. It was shown that the particular loading, unloading or reloading events can be simulated by introducing active loading and memory surfaces with proper slip rules similar to plastic flow and hardening rules associated with multisurface plasticity models.

In this work, we shall discuss the flexural behaviour of an elastic beam resting on a frictional foundation and acted on by an increasing force or moment inducing progressive slip zones propagating throughout the beam. The analysis becomes much more complex with respect to that of an elastic strip under tension since an infinite number of slip zones develop from the loaded boundary under monotonically increasing load. This problem was already analysed by Fischer, *et al.* (1991) and Fischer and Rammerstorfer (1991) who studied the deformation response of a beam on frictional foundation due to temperature gradient. They reported some technological problems arising during cooling of long rails after hot-rolling and provided the computational scheme based on a discretized beam model. Recently, the same problem was analysed by Nikitin (1992) who considered an infinite beam loaded by the lateral force and assumed an infinite number of slip zones obeying the self-similarity property. A closely related work by Zingone (1968) concerned with a beam on elastic, perfectly plastic Winkler foundation should also be mentioned. Our study extends the previous analyses of these authors and provides a uniform treatment for both monotonic and cyclic loading histories. It is important to note that in contrast to the solution for a tensile strip the cyclically varying load induces transient response tending asymptotically to a steady state.

The Coulomb friction condition and the non-associated slip rule neglecting contact dilatancy are used in the analysis. A so called "elastic" friction model for which beam deflection, not its rate, is associated with the friction force, is used in Section 6. For the case of monotonic loading, this model provides a simple closed form solution being a close approximation to the respective solution obtained for the slip rule. A general discussion of this model can be found in a book by Duvaut and Lions (1973). More complex slip or sliding rules developed by Mróz and Jarzębowski (1994) and Mróz and Stupkiewicz (1994) accounting for contact compliance and its state evolution could also be applied. The present

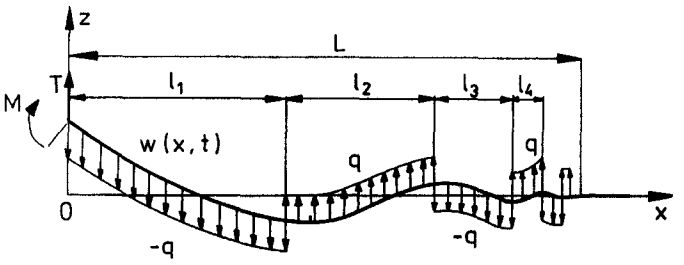

Fig. 1. Beam resting on the frictional foundation loaded at its tip by concentrated force T and moment M.

analysis, though simplified, provides an insight into the complex phenomena of contact interaction of flexural members such as beams, tubes or rails with frictional foundations. Such problems are typical in off-shore technology or in railway systems. The analysis can also be relevant in a study of shear delamination and frictional slip in composite structures.

2. PROBLEM FORMULATION

To make our analysis self-contained, we shall provide a detailed discussion and formulation applicable for both monotonic and variable loading. The specific case of proportional loading will be analysed in Section 5 as a particular case of the general formulation.

Let us consider an initially straight, elastic, semi-infinite beam resting on a rigid horizontal frictional foundation and loaded by the lateral force $T(t)$ and bending moment $M(t)$ at its tip, Fig. 1. When the beam deflects, lateral slips occur between the beam and the supporting foundation. External loading is then equilibrated by distributed friction forces. It is natural to expect and so it is assumed, that the deflection zone will not cover the whole beam length, but will propagate as the loading increases (the phenomena described by Fischer *et al.* (1991) confirm this assumption). We shall call the zone, in which deflections and therefore also contact slips occurred during the loading process, the deflection zone, and its length will be denoted by $L_d(t) < \infty$.

Further, it is assumed that the contact between the beam and the foundation occurs along the centre line. This implies that in each cross-section of the beam there is only one point in contact with the foundation and thereby no axial slips occur on contact due to rotations of the cross-sections. The torsion effect due to eccentric friction forces is neglected. Assuming the Coulomb friction condition between beam and foundation the equilibrium equation of the beam portion $0 \leqslant x \leqslant L_d$ under quasi-static loading is

$$EI_y w^{IV} = -q\,\widetilde{\operatorname{sign}}(\dot{w}), \tag{1}$$

with the boundary conditions

$$EI_y w''(0,t) = M(t), \quad EI_y w'''(0,t) = T(t) \tag{2}$$

and

$$w(L_d,t) = 0; \quad w'(L_d,t) = 0; \quad w''(L_d,t) = 0; \quad w'''(L_d,t) = 0 \tag{3}$$

and the initial condition:

$$w(x,0) = w_0(x) \equiv 0. \tag{4}$$

Here $w = w(x,t)$ denotes the lateral beam deflection, prime is the partial derivative with respect to x and dot denotes the derivative with respect to evolution (or time-like) parameter t. A non-unique function $\widetilde{\operatorname{sign}}(\dot{w})$ is defined by:

$$\dot{w} < 0: \quad \widetilde{\text{sign}}(\dot{w}) = -1;$$
$$\dot{w} = 0: \quad |\widetilde{\text{sign}}(\dot{w})| \leqslant 1;$$
$$\dot{w} > 0: \quad \widetilde{\text{sign}}(\dot{w}) = 1. \tag{5}$$

Boundary condition (2) could be replaced by respective conditions on beam tip rotation and deflection in case of displacement controlled loading.

Parameters of the system are the flexural stiffness EI_y and the limit friction traction $q = \gamma\mu$, where γ is the specific weight of beam per unit length and μ is the friction coefficient. In a general case all these quantities can vary along the beam length, but in the present formulation they are assumed as constant, so the problem is fully described by two parameters EI_y, q, and the loading history $T(t)$ and $M(t)$.

A simplified problem with elastic friction model instead of the classical Coulomb friction model can also be introduced. The elastic friction model (frequently applied in modelling contact friction) assumes that friction force depends on the sign of deflection, and not on the sign of deflection rate. However, since this model has no dissipation, it can only be used for monotonic loading. The beam equation now has the form

$$EI_y w^{IV} = -q\,\widetilde{\text{sign}}(w). \tag{6}$$

Equations (1)–(4) describe the quasi-static bending of an initially straight beam. Because of the expression $\widetilde{\text{sign}}(\dot{w})$, the partial differential eqn (1) is highly nonlinear and therefore no analytical solution is known to this problem. In the next section some considerations are presented, taking into account mechanical properties of the beam–foundation system, thus leading to an alternative formulation and, further, allowing for a numerical solution of the problem.

3. PROPERTIES OF THE BEAM–FOUNDATION INTERACTION

3.1. *Monotonic loading*

In this section some properties of the system will be discussed in case of monotonic loading. As it was already shown by Fischer *et al.* (1991) and Nikitin (1992), the initially straight beam after loading consists of two portions: the slip zone with non-zero deflection rate and the stick zone. The stick zone constitutes a part of the beam where no slips occurred during loading process: $w \equiv 0$, $x \geqslant L_s$; where L_s denotes the length of the slip zone.

Since the length of the slip zone can only increase as a function of monotonically increasing loading, the slip zone covers the whole length of the deflection zone, i.e. the portion of the beam where any deflection occurred during the loading process. It follows that for monotonic loading, there is no distinction between the slip zone and the deflection zone: $(L_s = L_d = L)$.

The slip zone $0 \leqslant x \leqslant L$ is assumed to consist of an unknown number of slip segments. Within each slip segment friction tractions $f(x, t)$ have the same orientation and the neighbouring segments with different friction force orientations are connected by points of vanishing slip velocity. In those points friction forces are indefinite, while in each slip segment the friction forces are constant and equal either to $+q$ or $-q$. In the stick zone, where no slips occurred during the loading process, obviously friction traction vanishes, $f(x, t) \equiv 0$.

Equation of the beam (1) can now be written:

$$EI_y w^{IV} = -q\,\text{sign}(\dot{w}), \tag{7}$$

where $\text{sign}(\dot{w})$ is now a unique function:

$$\dot{w} < 0: \quad \text{sign}(\dot{w}) = -1;$$
$$\dot{w} = 0: \quad \text{sign}(\dot{w}) = 0;$$
$$\dot{w} > 0: \quad \text{sign}(\dot{w}) = 1. \tag{8}$$

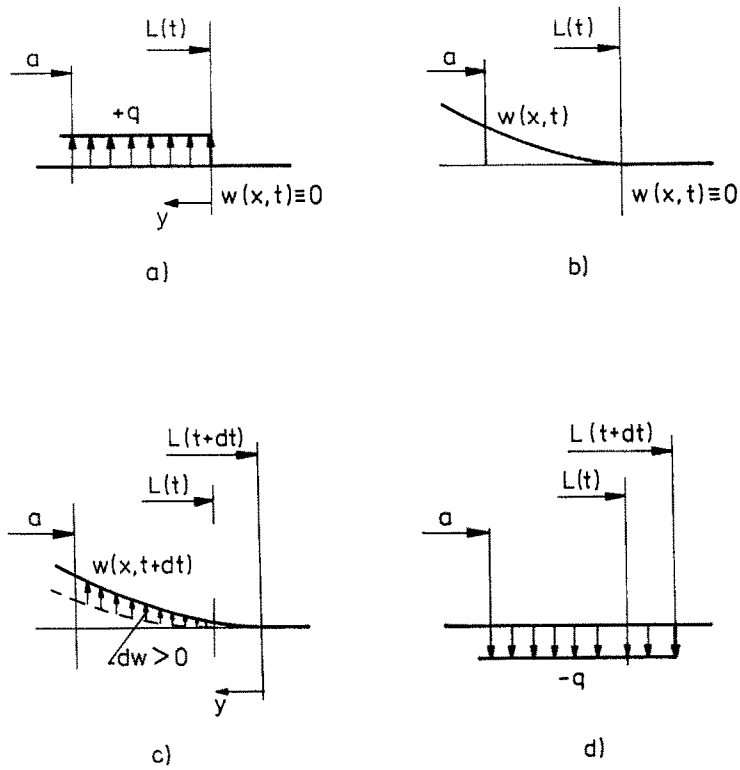

Fig. 2. Illustration to the proof of absence of solution consisting of a finite number of slip segments: (a) lateral segment loading; (b) deflection field; (c) slip field; and (d) lateral loading resulting from slip field.

The solution of eqn (7) must satisfy six boundary conditions (2) and (3). Assuming the number of slip segments to be equal to N we have $N-1$ additional conditions from the requirement of vanishing of slip velocity at the connecting points, between consecutive slip segments. The unknowns are: four integration constants of the differential eqn (7) and N lengths of the slip segments. Since altogether there are $N+4$ unknowns and $N+5$ equations, the conclusion can be drawn, cf. Nikitin (1992), that the solution cannot be found for any finite number N, but only an infinite set of slip segments can constitute a solution.

This overdetermination of the system of equations describing the problem leading to a solution with infinite number of equations can also be explained in mechanical terms. Assume that for some value of loading there exists a certain friction force distribution within a finite number of slip segments. Let us consider now the beam portion $a \leqslant x \leqslant L(t)$ being a part of the last slip segment, Fig. 2a. Accounting for the boundary conditions (3) and assuming positive friction force orientation $f(x,t) = q$ as in Fig. 2a, the deflection of the considered beam portion for the load parameter t and $t+\Delta t$ is drawn schematically in Fig. 2b and equals

$$w = \frac{q}{24EI_y} y^4 = \frac{q}{24EI_y}(L-x)^4. \tag{9}$$

Note, that since the length of slip zone grows monotonically, there is $L(t) < L(t+\Delta t)$. This implies velocity field of beam points in contact with foundation

$$\dot{w} = \frac{q}{6EI_y}(L-x)^3 \dot{L} > 0, \tag{10}$$

as shown in Fig. 2c and from the Coulomb's friction law we get friction force distribution $f(x,t) = -q\,\mathrm{sign}(\dot{w}) = -q < 0$, given in Fig. 2d, opposite to the assumed one. This proves

that it is impossible to satisfy both friction law and boundary conditions (3), if friction force distribution consists of a finite number of slip segments.

So, the infinite number of slip zones is the result of the one-dimensional model of the beam and of the Coulomb friction model. The model applied may loose its physical meaning when the slip zone lengths are of the order of dimensions of the cross-section and when the deflections are so small, that friction model with elastic contact compliance would be more relevant. However, this is the common problem of mathematical modelling of real structures and it means that the infinite number of slip segments is induced by a solution of the mathematical problem rather than by the physical reality.

The lengths of slip segments can be described by a convergent sequence l_i, which must fulfill the following conditions:

$$\lim_{i\to\infty} l_i = 0, \quad \lim_{i\to\infty} \sum_{k=1}^{i} l_k = \lim_{i\to\infty} J_i = L_s. \tag{11}$$

Here $J_i(t)$ denotes positions of the limits of the neighbouring slip segments:

$$J_i = \sum_{k=1}^{i} l_k. \tag{12}$$

3.2. *General loading*

In the general loading case, the division of the beam into slip and stick zones must be analysed more carefully. If for some loading history the length of the slip zone L_s would decrease, then equality of the slip and deflection zones would be no longer valid, because the deflection zone length L_d can never decrease. In such a case a region of frozen slips $L_s < x < L_d$ might form between the slip zone and the portion of the beam where no slips occurred during loading. In the frozen slips zone, friction force distribution $f(x, t)$ can have any value satisfying the inequality $|f(x, t)| \leqslant q$.

Equation (1) can be replaced by eqn (7) for the slip zone $0 \leqslant x \leqslant L_s$, but the boundary condition (3) must now be changed to

$$x = L_s: \quad w''' = \frac{d^3 w_f}{dx^3}, \quad w'' = \frac{d^2 w_f}{dx^2}, \quad w' = \frac{dw_f}{dx}, \quad w = w_f \tag{13}$$

where $w_f(x)$ is the frozen beam deflection in the stick zone $L_s < x < L_d$. If there is no region of frozen slips, then boundary conditions (13) are equivalent to (3), as it is for example in the monotonic loading case.

As discussed previously, there is a possibility, that a region of frozen slips forms between the slip zone and area where no slips occurred during loading. In such a case boundary conditions at $x = L_s$ are changed, eqn (13), making the problem unsolvable, because there are no relations allowing determination of the frozen deflection w_f. In order to enable solution, the following simplifying assumption is taken, namely that the frozen deflections are negligible:

$$w(x, t) \equiv 0, \quad x \geqslant L_s, \tag{14}$$

resulting in form (3) of boundary conditions at $x = L_s$ (L_d must be replaced by L_s in eqn (3)). Though no proof of this assumption for arbitrary loading exists, there are specific loading histories for which assumption (14) is true. There are also some reasons to believe that it is at least a good approximation. First of all, this assumption is automatically satisfied if the slip zone length L_s is a monotonically increasing function of the load parameter (time), because in such a case frozen deflections zone never occurs.

Now the question arises whether it is possible for the slip zone to shrink. It can be shown in a way similar to that illustrated in Fig. 2, that each load increment dT, dM must

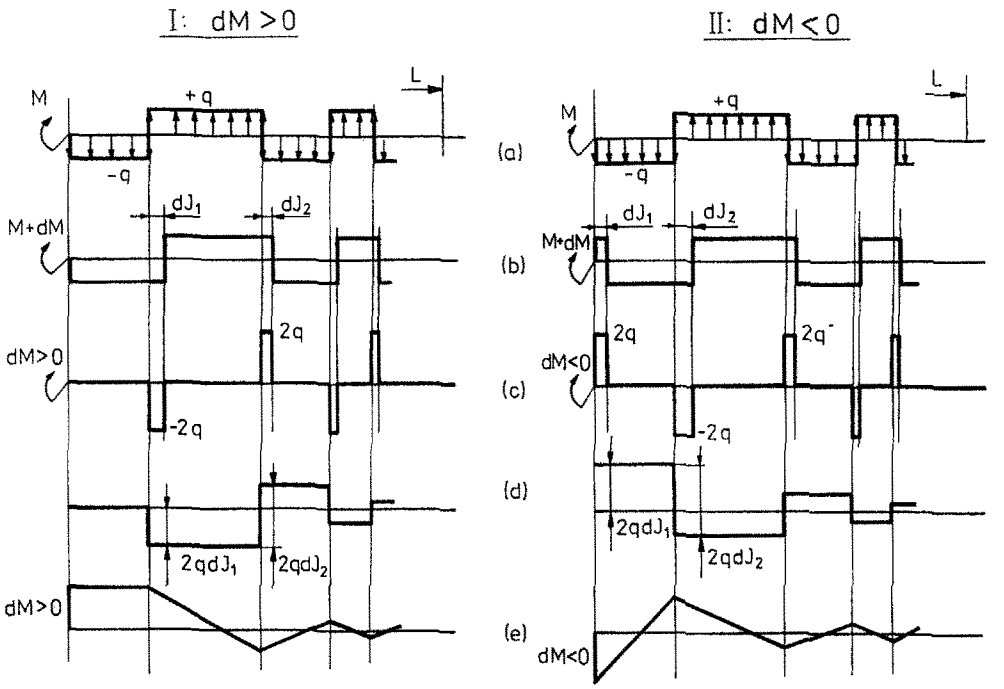

Fig. 3. Comparison of the friction force distribution of the beam loaded monotonically by the moment M subjected to load increments: I—positive (continued loading); and II—negative (onset of unloading): (a) load scheme for moment value M; (b) load scheme for moment value $M+\mathrm{d}M$; (c) distribution of increment of friction forces equilibrating load increment $\mathrm{d}M$; (d) distribution of increment of shearing force in the beam and (e) distribution of increment of bending moment in the beam. In (d) and (e), lengths of increments $\mathrm{d}J_i$ are neglected.

be accompanied by the change of lengths and positions of all slip segments. It means, that for instance, when unloading of the beam begins, there is no local unloading zone at the beam tip, but the unloading response covers the whole slip zone, so that all points O_i and thereby all slip segments change their positions.

Further, each change of the sign of load increment produces a new slip segment at the beam tip, because the slip direction of the tip changes. For example, during unloading, though the load is decreasing, the new slip segment grows. In Fig. 3 the expected layouts of slip segments and internal force distributions due to positive and negative load increments are presented for the beam loaded monotonically by the moment. Growth of the first slip segment causes those next to it to move apart from beam tip. At the same time, all those slip segments can shorten, but since the first slip segment grows, the resultant total length of slip zone L_s may either increase or decrease.

Let us now assume that the length of the slip zone decreases. Since the friction tractions change orientation in consecutive slip segments, the deflection curve is expected to have a wave-like shape with decreasing amplitude and wave length, both converging to zero. If we assume that for certain loading increment the slip zone increment ΔL_s is negative, in the region between previous and new positions of the end point of the slip zone there would be an infinite number of waves of initial deflection curve. Two cases should be considered now. The boundary conditions at the end of the slip zone would have to oscillate an infinite number of times, which seems impossible for monotonic loading increment, or the frozen slips would be infinitely small. From the first case it can be concluded that the slip zone should never shrink, from the second, that the assumption of zero deflection in the stick zone is accurate.

The above discussion shows that the assumption (14) should be a good approximation in the case when $\dot{L}_s < 0$ and it will be automatically satisfied when $\dot{L}_s \geqslant 0$. Also the numerical solutions of the problem, conducted under assumption (14), do not violate this assumption. As it will be discussed in later sections, it was observed that the total length of slip zone

$L_s(t)$ was monotonically growing for all treated loading cases. Moreover all functions of $J_i(t)$ never decreased, which means that the slip segments evolve in such a manner that their ends always move apart from the beam tip.

4. THE DEFLECTION CURVE

In this section the deflection curve of the beam will be found as a function of sequence of slip segment lengths l_i. The way to do it is basically similar to that presented by Fischer *et al.* (1991) and Nikitin (1992) with the main distinction that in the present formulation the infinite number of slip segments will be accounted for. The beam eqn (7) will be integrated within each slip segment and the solutions will be glued together in a way satisfying continuity of the deflection curve and its three derivatives and boundary conditions (3) for $x = L_s$. After applying the assumption (14) the point $x = L_s$ divides the whole beam into two distinct portions: the slip zone with non-zero deflection rates and the zone where deflection is zero ($w \equiv 0$ for $x \geqslant L_s$). Since this now is the only characteristic point of the beam, its length will be denoted by simply $L = L_s$.

Let us consider a slip segment in its local coordinate system $O_i x_i z_i$, Fig. 4. In this coordinate system the beam eqn (1) has the form

$$EI_y w^{IV} = n_1(-1)^{i-1}q, \quad 0 \leqslant x_i \leqslant l_i, \quad n_1 = \pm 1, \quad i = 1, 2, \ldots, \infty \tag{15}$$

where n_1 depends on friction force orientation in the first slip segment ($n_1 = 1$ when it is positive). The deflection curve of each segment can now be easily obtained

$$w_i(x_i) = \frac{1}{EI_y}\left[n_1\frac{(-1)^{i-1}}{24}qx_i^4 + \tfrac{1}{6}T_i x_i^3 + \tfrac{1}{2}M_i x_i^2\right] + \Theta_i x_i + W_i, \quad 0 \leqslant x_i \leqslant l_i \tag{16}$$

where

$$x_i = 0: \quad EI_y w_i''' = T_i, \quad EI_y w_i'' = M_i, \quad w_i' = \Theta_i, \quad w_i = W_i, \quad i = 1, 2, \ldots, \infty \tag{17}$$

are the boundary conditions of (16) at $x_i = 0$. Due to requirement of continuity of deflection curve and of static field we have

$$x_i = l_i: \quad EI_y w_i''' = T_{i+1}, \quad EI_y w_i'' = M_{i+1}, \quad w_i' = \Theta_{i+1}, \quad w_i = W_{i+1}, \quad i = 1, 2, \ldots, \infty. \tag{18}$$

The infinite sequences T_i, M_i, Θ_i and W_i must converge to zero when $i \to \infty$ to fulfill the global boundary conditions (3) for $x = L$. This is satisfied when condition (11) is valid and when these sequences are specified as

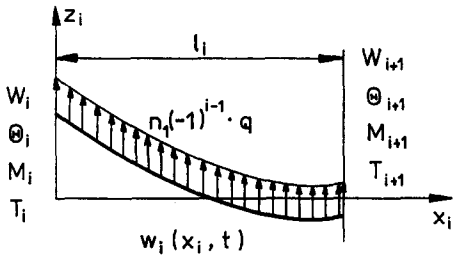

Fig. 4. Local coordinate system of the i-th slip segment.

$$T_i = \sum_{k=i}^{\infty} n_1(-1)^k q l_k,$$

$$M_i = \sum_{k=i}^{\infty} \left[n_1 \frac{(-1)^k}{2} q l_k^2 - T_k l_k \right],$$

$$\Theta_i = \frac{1}{EI_y} \sum_{k=i}^{\infty} \left[n_1 \frac{(-1)^k}{6} q l_k^3 - \tfrac{1}{2} T_k l_k^2 - M_k l_k \right],$$

$$W_i = \frac{1}{EI_y} \sum_{k=i}^{\infty} \left[n_1 \frac{(-1)^k}{24} q l_k^4 - \tfrac{1}{6} T_k l_k^3 - \tfrac{1}{2} M_k l_k^2 - EI_y \Theta_k l_k \right]. \tag{19}$$

The expressions subject to summation in (19) are simply the increments of respectively shearing force, bending moment, deflection slope and deflection over the slip segment k, resulting from the solution (16).

Boundary conditions (2) can be written as

$$T_1 = T(t), \quad M_1 = M(t). \tag{20}$$

The non-dimensional form of eqns (16)–(20) can easily be obtained by introducing the characteristic length l_0 and non-dimensional quantities:

$$l_i^* = \frac{l_i}{l_0}, \quad w^* = \frac{w}{(ql_0^4/EI_y)}, \quad T_i^* = \frac{T_i}{ql_0}, \quad M_i^* = \frac{M_i}{ql_0^2}, \quad \Theta_i^* = \frac{\Theta_i}{(ql_0^3/EI_y)}, \quad W_i^* = \frac{W_i}{(ql_0^4/EI_y)}. \tag{21}$$

With the use of eqns (16) and (19), the deflection curve $w(x, t)$ is described in terms of slip segment lengths $l_i(t)$. To complete the model, the segments l_i must be specified from the condition of vanishing rate of deflection at the connecting points. Note that the connecting points O_i separating segments l_{i-1} and l_i move along the beam during the progressive loading, thus their coordinates vary in time, $J_{i-1} = J_{i-1}(t)$. Therefore the convected time derivative should be used. Representing the beam deflection in terms of the local moving coordinate x_i

$$x = x_i + J_{i-1}, \quad w(x, t) = w_i(x_i, t) = w_i(x - J_{i-1}, t), \tag{22}$$

we have

$$\dot{w}|_{x=J_{i-1}} = \left.\frac{\partial w_i}{\partial t}\right|_{x_i=0} - \frac{\mathrm{d}J_{i-1}}{\mathrm{d}t} \left.\frac{\partial w_i}{\partial x_i}\right|_{x_i=0} = 0, \quad i = 2, 3, \ldots, \infty; \tag{23}$$

or in view of (19), these conditions take the form

$$\frac{\mathrm{d}W_i}{\mathrm{d}t} - \frac{\mathrm{d}J_{i-1}}{\mathrm{d}t} \Theta_i = 0, \quad i = 2, 3, \ldots, \infty. \tag{24}$$

This infinite set is in fact a set of differential equations, since it can be presented in a form

$$\sum_{j=1}^{\infty} A_j^i \frac{\mathrm{d}l_j}{\mathrm{d}t} = 0, \quad i = 2, 3, \ldots, \infty; \tag{25}$$

where

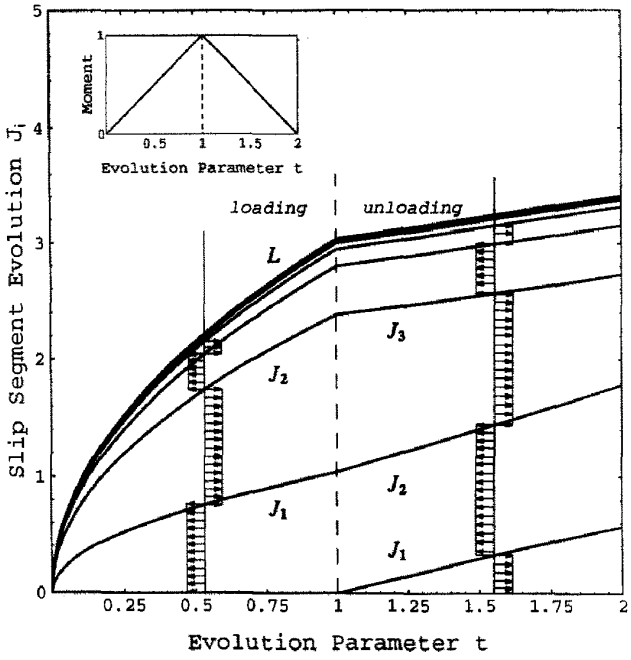

Fig. 5. Typical slip segment evolution diagram, $J_i^*(t)$. Curve with the highest value is the total length of the slip zone $L^* = J_\infty^*$. The friction force distribution for certain loading and unloading points is presented.

$$A_j^i = A_j^i(l_k) = \frac{\partial W_i}{\partial l_j} - \Theta_i \frac{\partial J_{i-1}}{\partial l_j}, \quad i = 2, 3, \ldots, \infty, \quad j,k = 1, 2, \ldots, \infty. \tag{26}$$

The conditions (23) hold for $i = 2, 3, \ldots, \infty$, that is at all points separating slip segments except at the beam tip, because there is no condition limiting deflection rate at this point. However, once during the loading process the beam tip velocity becomes zero and next changes its orientation, it means, that a new slip segment has been created (cf. Fig. 5). In such a case the slip segments must be renumbered and their values are set to

$$\begin{aligned} l_i &:= l_{i-1}, \quad i = 2, 3, \ldots, \infty \\ l_1 &:= 0 \\ n_1 &:= -n_1. \end{aligned} \tag{27}$$

The initial problem specified by the nonlinear partial differential eqn (1) with boundary conditions (2) and (3) has been reformulated after some features of the friction problem considered have been used. The infinite set of differential eqns (25) with two additional algebraic eqns (20) describes evolution of slip segment lengths $l_i(t)$ of the beam loaded at the tip by lateral force $T(t)$ and bending moment $M(t)$. In view of initial condition (4) the initial values of $l_i(t)$ are

$$l_i(0) = 0, \quad i = 1, 2, \ldots, \infty. \tag{28}$$

Although such a problem has no analytical solution in any of two formulations, the second form is suitable for numerical treatment. In the following sections, some approximations and solution methods will be presented for monotonic proportional loading and next for arbitrary loading.

5. PROPORTIONAL LOADING

The specific case of loading will now be considered, namely monotonic proportional loading. It was shown by Nikitin (1992), that in case of monotonically increasing loading the solution appears to be self-similar. Due to self-similarity the set of differential eqns (24) can be replaced by a set of algebraic equations. In this section the proper condition of proportional loading will also be defined and an interesting feature of the solution will be shown.

In the simplest case the self-similar solution will be obtained when the beam is loaded only by one monotonically growing external load (i.e. lateral force T or bending moment M), while the other load is equal to zero. The characteristic length l_0 being a scaling reference length along the beam can be introduced, depending on the applied load:

$$l_0 = l_T = T/q \quad \text{or} \quad l_0 = l_M = \sqrt{M/q}. \tag{29}$$

The self-similar solution can also occur when both force and moment are applied, but the following condition of self-similarity must be satisfied:

$$\frac{l_T}{l_M} = \text{const.} \tag{30}$$

The above condition expressed in terms of loads is the definition of proportional loading:

$$\frac{T^2}{M} = \text{const.} \tag{31}$$

The self-similar solution in the case of proportional monotonic loading is specified in terms of the non-dimensional sequence l_i^*. The slip segment evolution is then given by

$$l_i(t) = l_i^* l_0(t), \tag{32}$$

where l_0 is now monotonically growing with increasing load and all non-dimensional quantities do not depend on time.

For proportional loading the conditions (24) can be transformed to

$$(4W_i^* - J_{i-1}^* \Theta_i^*) l_0^3 \frac{\mathrm{d}l_0}{\mathrm{d}t} = 0, \quad i = 2, 3, \ldots, \infty, \tag{33}$$

which are satisfied when

$$4W_i^* - J_{i-1}^* \Theta_i^* = 0, \quad i = 2, 3, \ldots, \infty. \tag{34}$$

Conditions (34) of vanishing deflection rates are fully consistent with those obtained by Nikitin (1992). These equations together with boundary conditions (20) in the non-dimensional form constitute an infinite set of nonlinear algebraic equations with unknown infinite sequence l_i^*.

No analytical solution is known to this problem, so an approximate numerical solution can only be constructed. However, an interesting feature of the system can be found if the following form of geometric sequence of l_i^* is assumed:

$$l_{i+1} = e l_i, \quad i \geqslant i_e, \quad 0 < e < 1. \tag{35}$$

The non-dimensional series T_i^*, M_i^*, Θ_i^* and W_i^* also becomes the geometric series for $i \geqslant i_e$ and the following relations hold:

$$\Theta^*_{i+1} = -\Theta^*_i e^3, \quad W^*_{i+1} = -W^*_i e^4. \tag{36}$$

It is seen that geometric series W^*_iconverges to zero more quickly than $\Theta^*_i(e^4 < e^3)$. At the same time, as i increases, sequence J^*_iapproaches its limit L, eqn (11). It follows now that for $i \to \infty$ condition (34) can be reduced to

$$\Theta^*_i = 0 \quad \text{for } i \to \infty. \tag{37}$$

If we remember that $\Theta^*_i$is the slope at $x_i = 0$, the physical meaning of eqn (37) is that for i tending to infinity, points of vanishing deflection rate coincide with points in which the deflection curve reaches its extremal values. Equation (37) can be solved for e giving:

$$e = \lim_{i \to \infty} \frac{l_{i+1}}{l_i} = \frac{3-\sqrt{5}}{2} = 0.38197. \tag{38}$$

The following conclusion can be drawn from above considerations, that in case of monotonic loading, slip segment lengths l^*_iform a convergent sequence, which for $i \to \infty$ is "nearly" a geometric sequence. This feature of self-similar solution will be used in reducing the number of unknowns in the numerical solution of the problem.

6. ELASTIC FRICTION MODEL

A modification of the original problem will now be briefly discussed in order to provide a simple closed form solution. Namely, the elastic friction model will be used instead of the classical Coulomb friction model as it was formulated in Section 2, cf. eqn (6).

Now, the condition of vanishing deflection rate must be replaced by the condition of zero deflection in points O_i separating slip segments. For monotonic loading it has a simple form:

$$W^*_i = 0, \quad i = 2, 3, \ldots, \infty. \tag{39}$$

These equations are satisfied for l^*_iin a form of geometric series, eqn (35), with

$$e = \frac{l^*_{i+1}}{l^*_i} = \tfrac{1}{4}(3+\sqrt{33}-\sqrt{2}\sqrt{3\sqrt{33}+13}) = 0.2421, \quad i \geqslant i_e = 2. \tag{40}$$

The remaining l^*_1 and l^*_2 needed to complete the solution have to be found from the boundary conditions (20). As a result the following closed form analytical solution is obtained:

$$l^*_1 = T^* + \sqrt{1+e^2}\sqrt{0.5T^{*2}+M^*}, \quad l^*_2 = (1+e)(l^*_1 - T^*);$$

$$L^* = l^*_1 + \frac{1}{1-e} l^*_2;$$

$$\Theta^* = -\tfrac{1}{6}l^{*3}_1 + \tfrac{1}{2}T^* l^{*2}_1 + M^* l^*_1 + \frac{e^2-3e+1}{6(1+e^2)(1+e^3)} l^{*3}_2;$$

$$W^* = \tfrac{1}{24}l^{*4}_1 - \tfrac{1}{6}T^* l^{*3}_1 - \tfrac{1}{2}M^* l^{*2}_1 + \Theta^* l^*_1. \tag{41}$$

This solution is valid when the orientation of friction forces in the first slip segment is negative. This condition will be discussed and the results will be presented in Section 8.1 together with the results obtained for the classical Coulomb friction model.

7. APPROXIMATE SOLUTIONS

The problem formulated in previous sections has no analytical solution due to an infinite number of equations and unknowns. The main idea of the proposed method of numerical solution is to reduce the number of both. First of all, it is assumed that an infinite sequence of slip segment lengths l_i^* can be approximated using n parameters r_j:

$$l_i^* = l_i^*(r_j), \quad i = 1,2,\ldots,\infty, \quad j = 1,2,\ldots,n. \tag{42}$$

It is obvious that with increasing n the accuracy will be improved. Having in mind that sequence l_i^* is close to geometric series for i large enough, cf. Section 5, a very simple form of relation (42) was used, namely

$$\begin{aligned} l_i &= r_i \quad \text{for } 1 \leqslant i \leqslant n-1, \\ l_i &= r_n l_{i-1} \quad \text{for } i \geqslant n. \end{aligned} \tag{43}$$

The number of equations can be reduced simply by neglecting all deflection rate eqn (24) for $i > m+1$. It means, that only the first m of those equations are taken into account.

In the case of proportional monotonic loading the solution for given load parameters T^* and M^* can be found as a minimization problem

$$\min_{r_j} \sum_{k=1}^{m+2} w_k [f_k(r_j)]^2, \tag{44}$$

where w_k denote weight factors and f_k are the residual functions:

$$\begin{aligned} f_k(r_j) &= 4W_{k+1}^* - J_k^* \Theta_{k+1}^*, \quad k = 1,2,\ldots,m \\ f_{m+1}(r_j) &= T^* - T_1^* \\ f_{m+2}(r_j) &= M^* - M_1^*. \end{aligned} \tag{45}$$

In a general load case the self-similar solution is no longer valid and the condition of vanishing deflection rate has the form of differential eqn (25). The solution will provide the evolution of slip segments specified in terms of the evolution of parameters r_j. Again, only the first m eqns (25) are taken into account and in view of eqns (26) and (42) evolution equations have the form

$$\sum_{j=1}^{n} a_j^i \dot{r}_j = 0; \quad i = 2,3,\ldots,m+1 \tag{46}$$

where

$$a_j^i = a_j^i(r_k) = \sum_{s=1}^{\infty} A_s^i \frac{\partial l_s^*}{\partial r_j} = \frac{\partial W_i^*}{\partial r_j} - \Theta_i^* \frac{\partial J_{i-1}^*}{\partial r_j}, \quad i = 2,3,\ldots,m+1, \quad j = 1,2,\ldots,n. \tag{47}$$

Since the boundary conditions (20) are algebraic equations they can be differentiated in order to obtain uniform formulation, namely

$$\sum_{j=1}^{n} b_j^1 \dot{r}_j = \dot{T}^*, \quad \sum_{j=1}^{n} b_j^2 \dot{r}_j = \dot{M}^* \tag{48}$$

where

$$b_j^1 = \frac{\partial T_1^*}{\partial r_j}, \quad b_j^2 = \frac{\partial M_1^*}{\partial r_j}. \tag{49}$$

In eqns (46)–(49), the dot denotes time derivative and all quantities are made non-dimensional by using the time independent reference length l_0.

The evolution of parameters $r_j(t)$ is now found by numerical integration of incremental equations $\dot{r}_j = \dot{r}_j(r_j, t)$, which are determined in a manner similar to that proposed for the proportional loading case, namely

$$\min_{\dot{r}_j} \sum_{k=1}^{m+2} w_k [g_k(\dot{r}_j, r_j, t)]^2 \tag{50}$$

where w_k are weight factors and g_k stand for residual functions given by

$$g_k(\dot{r}_j, r_j, t) = \sum_{j=1}^{n} a_j^{k+1} \dot{r}_j, \quad k = 1, 2, \ldots, m$$

$$g_{m+1}(\dot{r}_j, r_j, t) = \sum_{j=1}^{n} b_j^1 \dot{r}_j - \dot{T}^*,$$

$$g_{m+2}(\dot{r}_j, r_j, t) = \sum_{j=1}^{n} b_j^2 \dot{r}_j - \dot{M}^*. \tag{51}$$

The initial values of $r_j(t)$ are needed for integration of $\dot{r}_j = \dot{r}_j(r_j, t)$ and here solutions of the respective proportional loading cases can be used.

Two kinds of phenomena that can occur during the loading process need special attention. As it was already discussed in Section 4, the velocity of the beam tip must be checked in each time step in order to find time at which new slip segment appears at the tip (for example in cyclic loading case this will happen only at each load reversal point). Moreover, the sequence l_i^*must be examined in order to check for vanishing slip segments. It may happen during loading that the length of a slip segment becomes zero. Then other slip segments must be renumbered and respective conditions (46) must be deleted.

8. RESULTS AND DISCUSSION

Some results of numerical calculations will now be presented. Semi-similar solutions of beam loaded by the lateral force and moment are shown in Fig. 6. Calculations for general load cases were performed only for the case $T = 0$. Figures 7–12 present evolution of slip segments $J_i^*(t)$ for different loading programs specified in terms of the applied moment $M^*(t)$, namely loading, unloading, reloading and cyclic loading. Since only quasi-static processes are of interest, in all cases moment was taken as a linear function of the load parameter t, increasing or decreasing depending on the loading event. The discontinuity of moment time derivative at reversal points has also no effect due to the same assumption. In all numerical examples, except for monotonic loading cases, the characteristic length l_M was related to the value of moment M_1 at the first reversal point, i.e. at the end of semi-similar solution. Of course, it follows that $M_1^* = 1$.

In order to analyse the hysteretic effects, the proper displacement measure related to external loading by moment M^* must be chosen, namely the beam tip rotation. It will be denoted by $\Theta^* = -\Theta_1^*$ to provide positive displacement for positive load.

The solution results are demonstrated by presenting the layout or evolution of the slip segments in cases of self-similar or general solutions, respectively. Positions of points of vanishing deflection rate O_i, namely $J_i^*(t)$, and the total length of the slip zone L^*, are presented in Fig. 5 for the simple case of loading–unloading program.

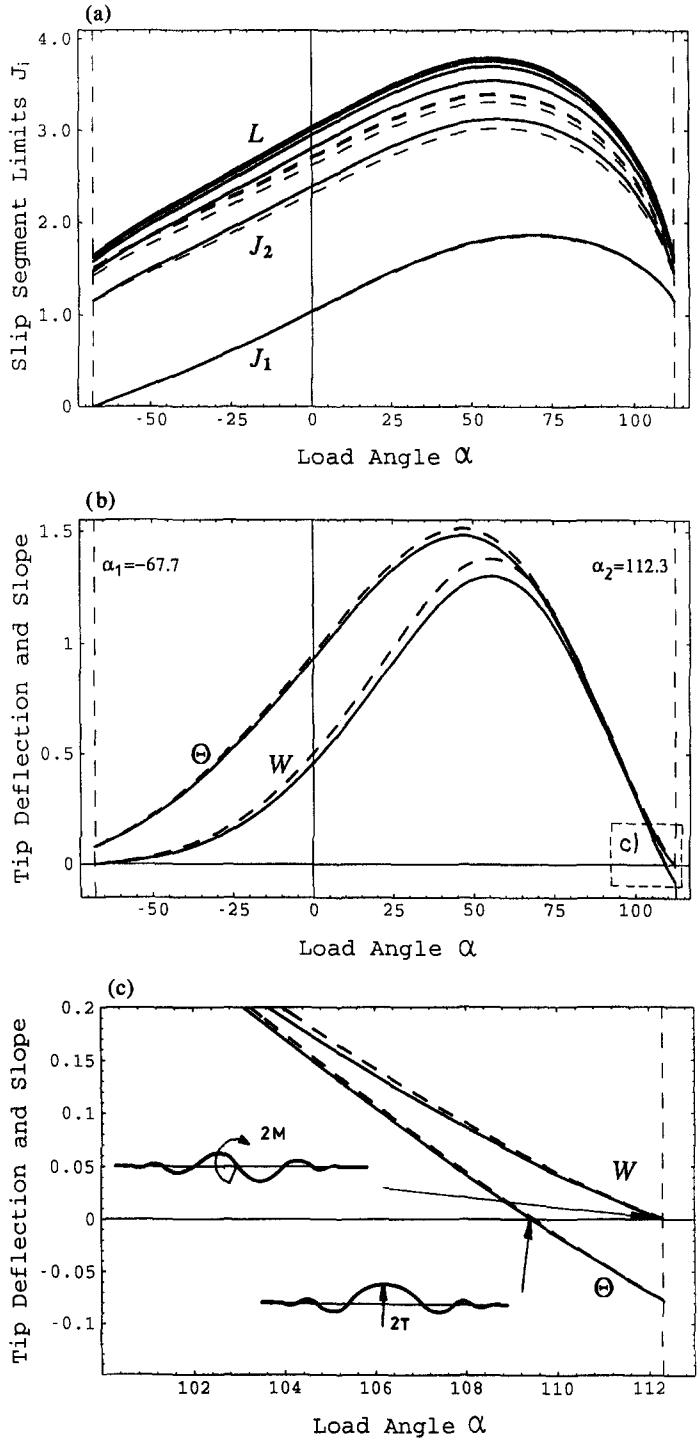

Fig. 6. Self-similar solutions of beam loaded monotonically by force T^* and moment M^* defined by a "load angle" α, eqn (57): (a) slip segment layout $J_i^*(\alpha)$; (b) beam tip deflection $W^*(\alpha)$ and rotation $\Theta^*(\alpha)$; and (c) solutions for an infinite beam loaded by force or moment. Results of elastic friction model are plotted with the dashed lines.

8.1. *Proportional loading*

Solutions of the beam under proportional monotonic loading depend only on one parameter, namely the proportionality factor between force and moment, eqn (29) or (30). For computational efficiency it was replaced by a "load angle" α:

$$T^* = \sin(\alpha), \quad M^* = \cos(\alpha) \tag{52}$$

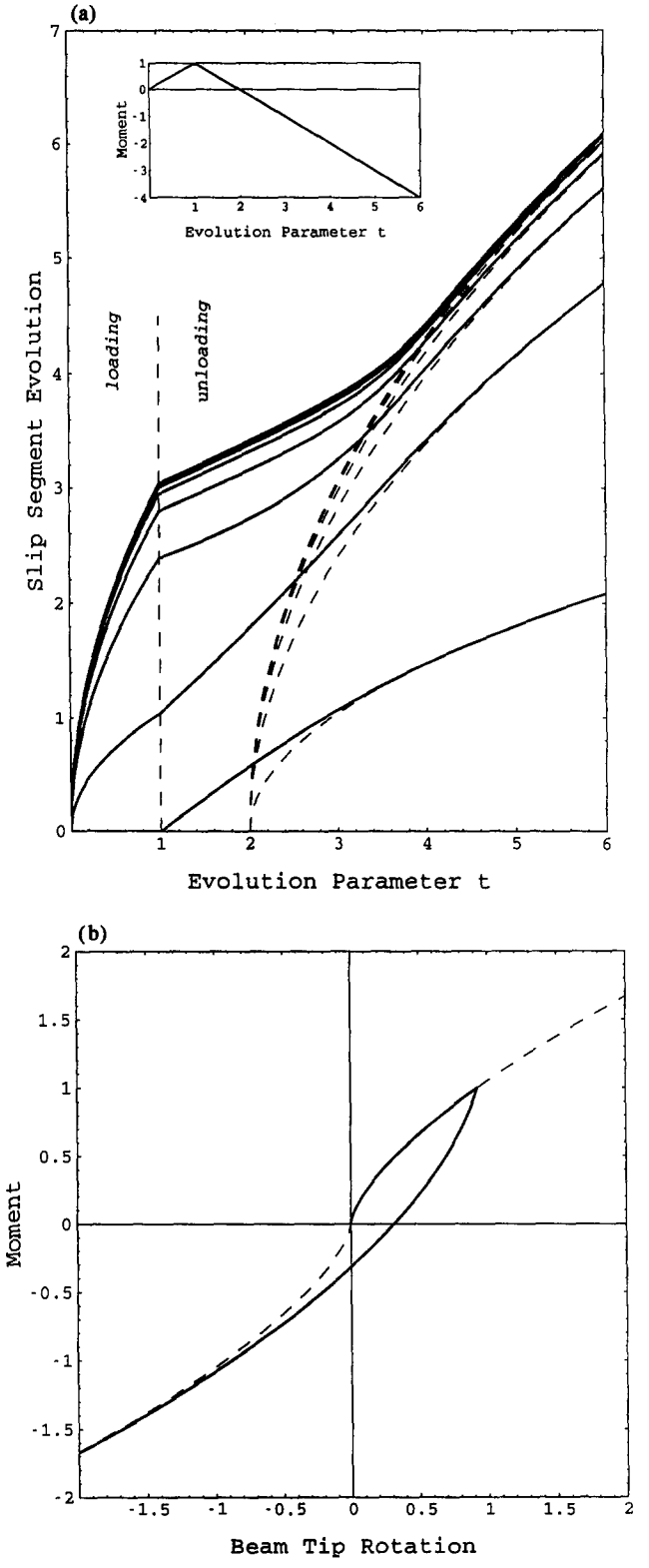

Fig. 7. Loading–unloading program, beam loaded by moment only ($T^* = 0$): (a) slip segment evolution $J_1^*(t)$; (b) load–displacement curve (moment M^* versus beam tip rotation Θ^*). Dashed lines denote self-similar solution for corresponding values of moment M^*.

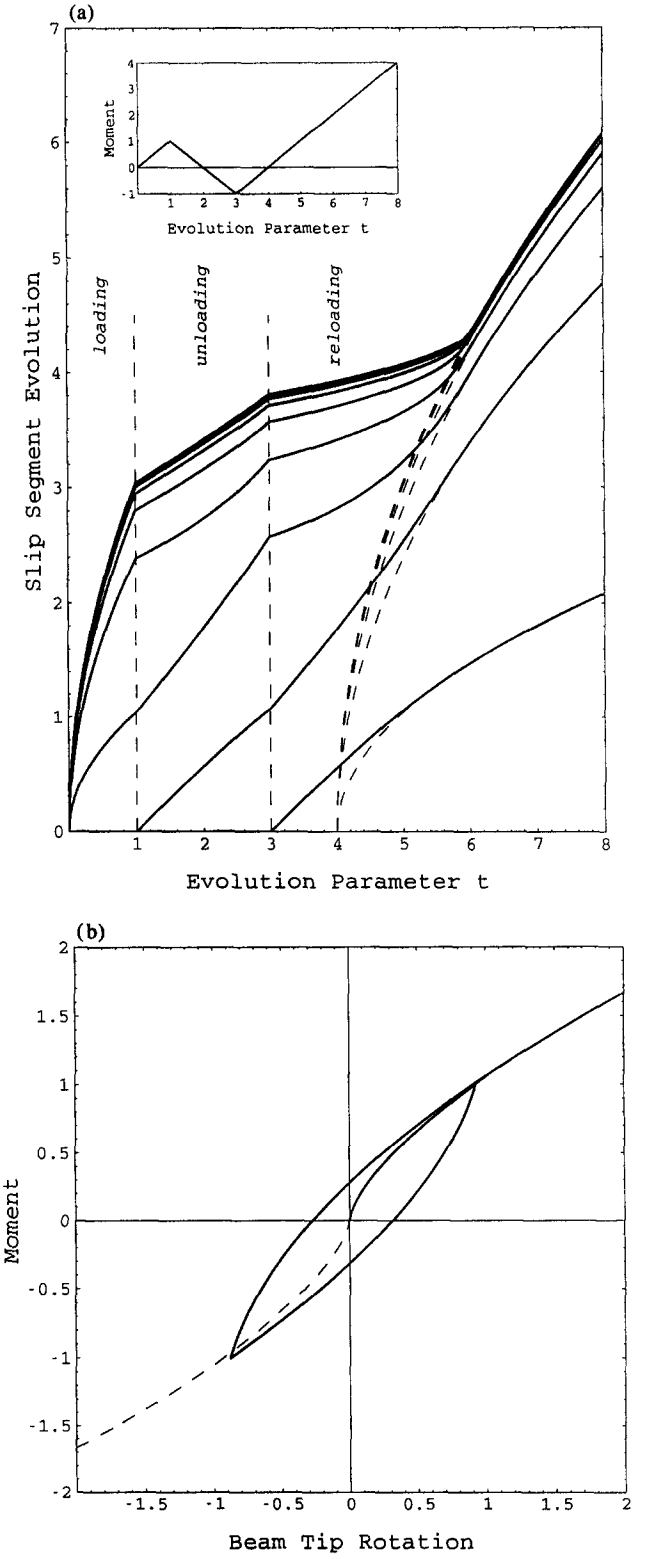

Fig. 8. Loading–unloading–reloading program, beam loaded by moment only ($T^* = 0$): (a) slip segment evolution $J_1^*(t)$; and (b) load–displacement curve (moment M^* versus beam tip rotation Θ^*). Dashed lines denote self-similar solution for corresponding values of moment M^*.

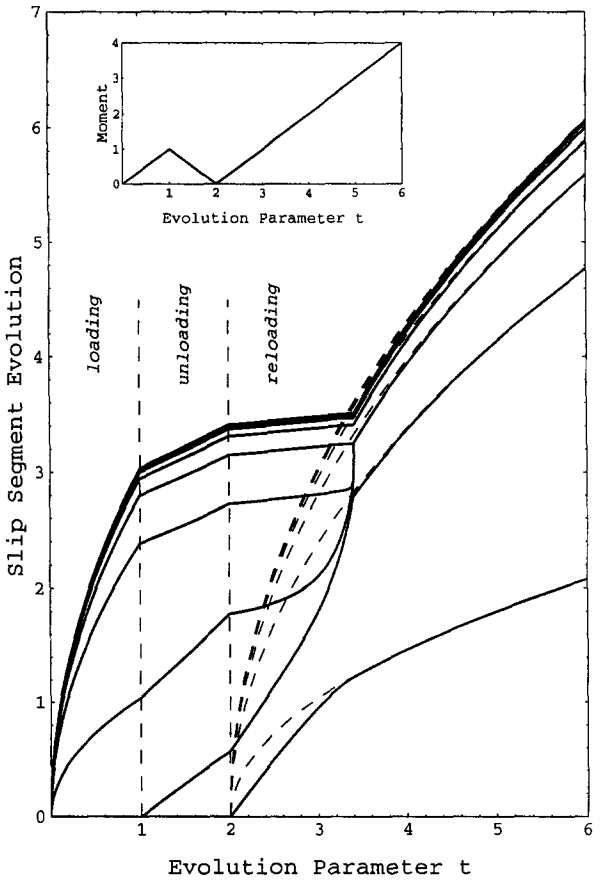

Fig. 9. Non-symmetric loading–unloading–reloading program, beam loaded by moment only ($T^* = 0$): slip segment evolution $J_i^*(t)$. Dashed lines denote self-similar solution for corresponding values of moment M^*.

which implies the characteristic length l_0 (expressed in terms of l_T and l_M, eqn (29)) in the form

$$l_0^2 = \tfrac{1}{2}(l_T^2 + \sqrt{l_T^4 + 4l_M^4}). \tag{53}$$

The cases of beam loaded by moment only and by force only are specified by $\alpha = 0°$ and 90°, respectively. In those cases the characteristic length l_0 equals l_M or l_T, respectively. The results are presented in Fig. 6, where diagrams $J_i^*(\alpha)$, $L^*(\alpha)$, $W_i^*(\alpha)$ and $\Theta_i^*(\alpha)$ are shown. The dashed lines denote analytical solution for the elastic friction model, cf. Section 6. The accuracy of this simplified model appears to be very good, especially when deflection of the beam tip is considered, Fig. 6b. Also the lengths of the first and second slip segments are not much different, but the total length of the slip zone differs of about 10%, Fig. 6a.

The parameter α varies from $\alpha_1 = -67.7°$ to $\alpha_2 = 112.3°$, and this is the range in which deflection of the beam tip is positive, Fig. 6b, and the friction forces orientation in the first slip segment is negative.

The limit values of α specify a case when the beam tip has no deflection. This case is equivalent to a case of an infinite beam loaded by the bending moment 2M, cf. Fig. 6c. The lateral force T can then be regarded as the reaction of one part of the beam on the other when only half of the beam is considered. For $\alpha_2 < \alpha < \alpha_1 + 180°$, the deflection of the tip is negative, while slip segment lengths are the same as for $\alpha - 180°$. It is also seen in Fig. 6a, that $J_i(\alpha_2) = J_{i+1}(\alpha_1)$.

The other similar loading case is specified by $\alpha = 109.4°$, namely an infinite beam loaded by the lateral force $2T$, Fig. 6c. Due to symmetry there is $\Theta_1 = 0$. The same case

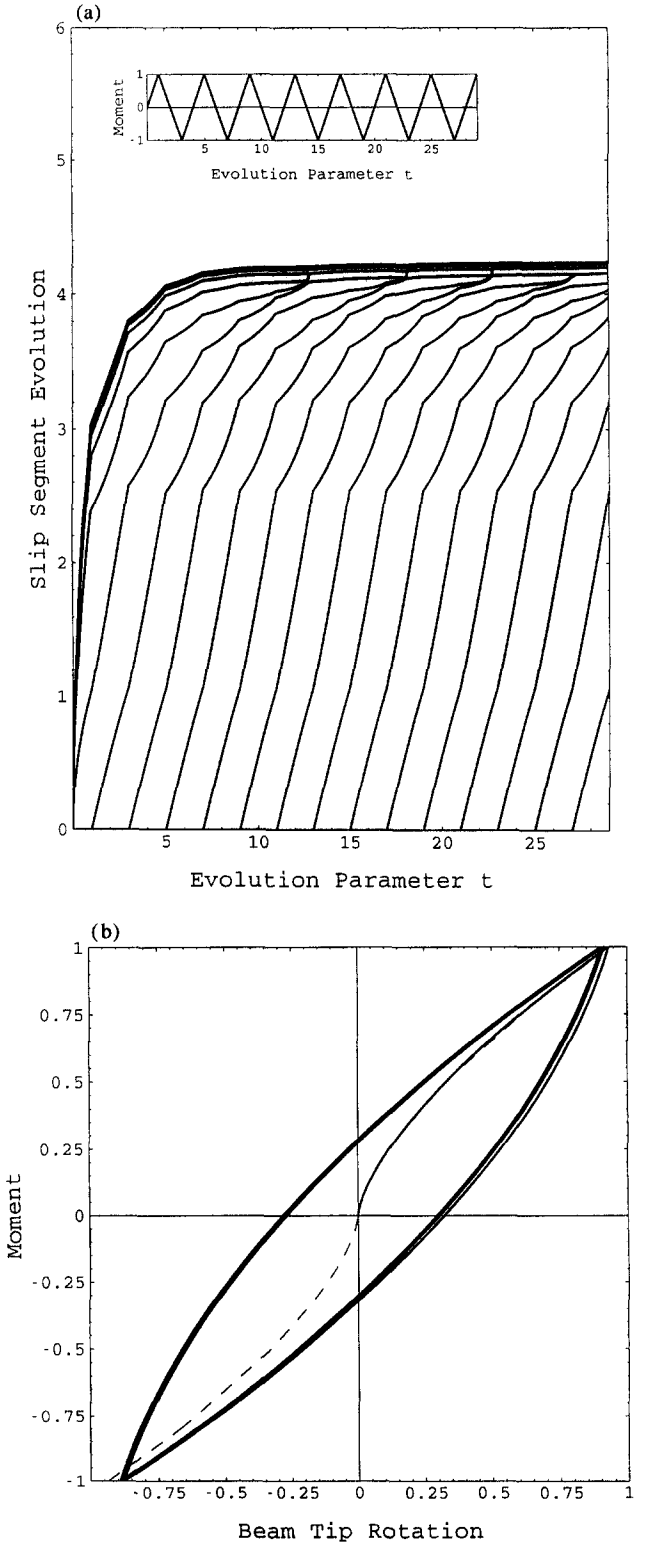

Fig. 10. Cyclic loading program, beam loaded by moment only ($T^* = 0$): (a) slip segment evolution $J_i^*(t)$ and (b) load–displacement hysteresis loop (moment M^* versus beam tip rotation Θ^*).

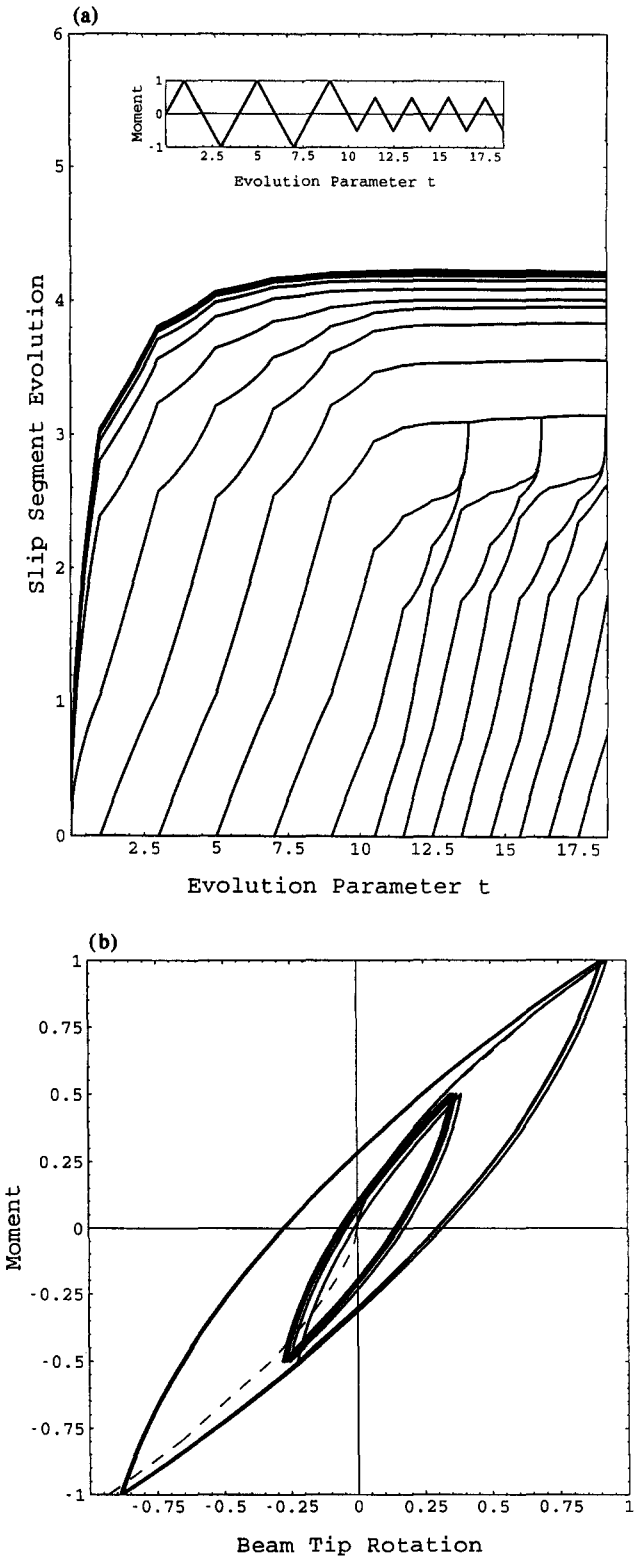

Fig. 11. Cyclic loading program with changing load amplitude, beam loaded by moment only ($T^* = 0$): (a) slip segment evolution $J_i^*(t)$; (b) load–displacement hysteresis loop (moment M^* versus beam tip rotation Θ^*); and (c) beam tip rotation in load reversal points (Θ^* for $M^* = 0.5$ and $-\Theta^*$ for $M^* = -0.5$).

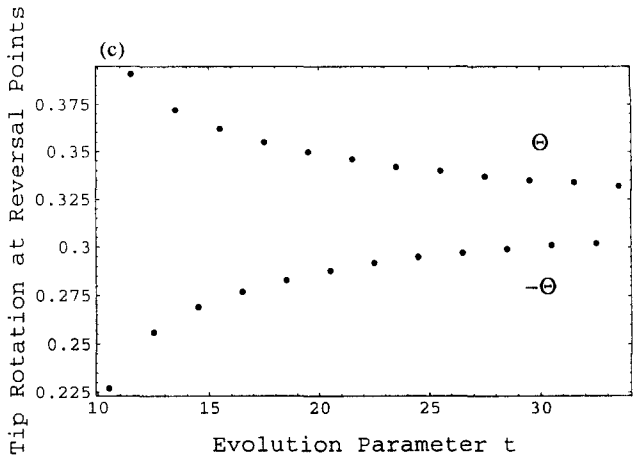

Fig. 11 *Continued.*

was solved by Nikitin (1992) and both results show very good agreement cf. Table 1, though the solution methods were different. Here the characteristic length was $l_0 = l_T$ and thereby $T^* = 1$.

The solution for the case of moment loading ($\alpha = 0$) can be identified with the solution for a free beam resting on the frictional foundation and subjected to the uniform initial curvature field $\kappa_i = \kappa_i(t)$ induced, for instance, by the temperature gradient. This case was studied by Fischer *et al.* (1991) in relation to the rail cooling problem. In fact, the field of moments $M^t(x, t)$ for this case can be generated from the field $M(x, t)$ obtained in this paper by writing

$$M^t(x, t) = M(x, t) - M^0(t) \tag{54}$$

where $M^0 = EI_y\kappa_i$. The sizes of slip segments and the deflection field in both cases are same.

In order to check the accuracy of our method, a solution of beam loaded by moment only ($\alpha = 0$) was determined for different values of approximation parameters m and n. The results presented in Table 2 indicate that the best accuracy was achieved when $n = m+2$. For bigger values of n the accuracy decreases, but it is still very good. Probably the reason for this is of numerical nature, namely that it is more difficult to find the minimum when the number of independent variables of minimized function increases. It is seen however, that the results are practically the same for a wide range of parameters m and n, cf. Tables 2 and 3.

It is also seen that the calculated value of r_n, which is the ratio of lengths of neighbouring slip segments for $i > n$, is in a very good agreement with the theoretical value in infinity, eqn (38).

Note that the total error (minimized norm of residual functions, eqn (44)) can only be compared for the same value of parameter m, i.e. the number of accounted conditions of vanishing deflection rate.

8.2. *Loading–unloading and loading–unloading–reloading programs*

Figures 7 and 8 present basic loading–unloading and loading–unloading–reloading programs, respectively. Unloading begins when $M_I^* = 1$, reloading when $M_{II}^* = -1$. It is seen, that in both cases, when load is increased, the memory of contact is gradually erased and the solution tends to a self-similar solution (dashed lines on Figs 7 and 8).

An interesting feature of the system can be observed in Fig. 9. If the reloading starts at the reversal point of the moment $M_{II}^* = 0$, two neighbouring slip segments disappear. This case is different from symmetric reloading, Fig. 8, where all slip segments evolve to semi-similar solution with increasing load. There must be a value of M_{II}^* separating these two kinds of solutions.

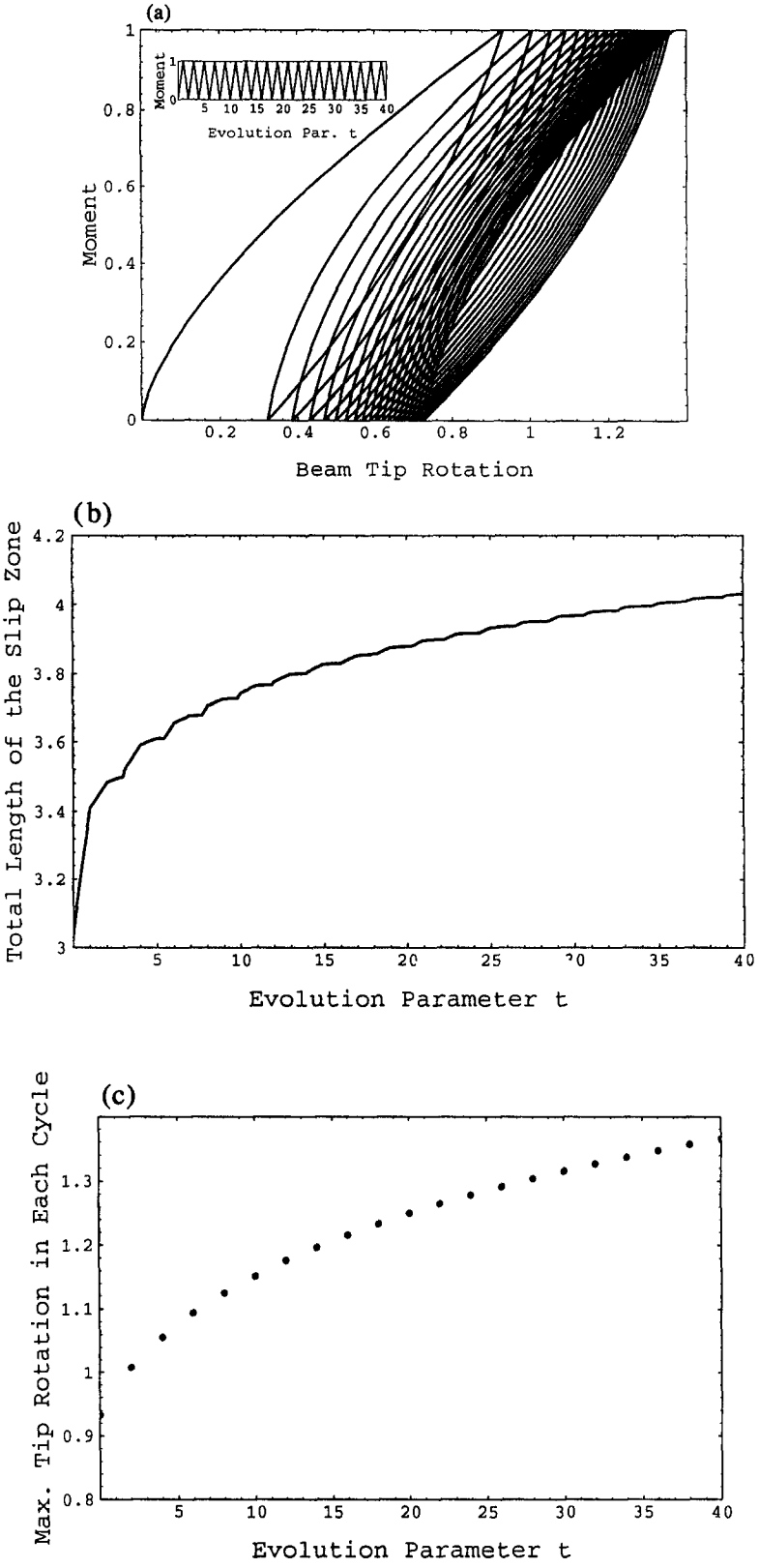

Fig. 12. Non-symmetric cyclic loading program, beam loaded by moment only ($T^* = 0$): (a) load–displacement hysteresis loop (moment M^* versus beam tip rotation Θ^*); (b) total length of the slip zone $L^*(t)$; and (c) maximum beam tip rotation in each cycle (for $M^* = 1$).

Table 1. Results for $\Theta_1 = 0$, compared with results of Nikitin (1992)

	M^*	W_1^*	$l_1^* = J_1^*$	J_2^*	$L^* = J_\infty^*$
Present solution	−0.3739	0.0684	1.3739	1.8725	2.1434
Nikitin (1992)	−0.374	0.068	1.374	1.873	2.141

Table 2. Results obtained for different values of parameter n for the case of moment loading ($\alpha = 0$)

m	n	l_1^*	l_2^*	l_3^*	$r_n = \frac{l_{i+1}^*}{l_i^*}$	L^*	Θ_1^*	Error
2	3	0.9269	1.2293	—	0.29381	2.6676	−0.68428	0.99×10
2	4	1.0407	1.3460	0.41214	0.35007	3.0208	−0.93296	0.56×10^{-29}
2	5	1.0407	1.3461	0.41363	0.37752	3.0399	−0.93297	0.11×10^{-28}
8	9	1.0405	1.3459	0.41316	0.38184	3.0365	−0.93259	0.11×10^{-1}
8	10	1.0407	1.3461	0.41324	0.38188	3.0370	−0.93296	0.10×10^{-14}
8	11	1.0407	1.3461	0.41324	0.38200	3.0370	−0.93296	0.44×10^{-11}

Table 3. Results obtained for different values of parameter m for the case of moment loading ($\alpha = 0$)

m	n	l_1^*	l_2^*	l_3^*	$r_n = \frac{l_{i+1}^*}{l_i^*}$	L^*	Θ_1^*	Error
2	8	1.0407	1.3460	0.41235	0.38235	3.0326	−0.93296	0.21×10^{-19}
4	8	1.0407	1.3461	0.41324	0.38213	3.0367	−0.93296	0.23×10^{-18}
6	8	1.0407	1.3461	0.41324	0.38134	3.0370	−0.93296	0.49×10^{-21}
8	8	1.0397	1.3451	0.41277	0.38180	3.0342	−0.93095	0.62×10^{-1}
10	8	1.0387	1.3441	0.41233	0.38193	3.0315	−0.92904	0.12×10

Table 4. Relative error of the method in the case of vanishing of slip segments for two different pairs of parameters m and n

t	$\Delta\Theta_1^*$ (%)	ΔW_1^* (%)	ΔL^* (%)	ΔJ_1^* (%)	ΔJ_2^* (%)	ΔJ_3^* (%)	ΔJ_4^* (%)	ΔJ_5^* (%)
2.40	−0.228	−0.376	0.029	−0.0001	−0.004	0.004	0.001	0.014
2.41	−0.226	−0.371	0.030	−0.0001	−0.006	0.293	0.292	0.014
2.43	−0.190	−0.378	−0.036	−0.065	−0.046	−0.097	−0.097	−0.097
5.00	−0.066	−0.109	−0.088	−0.035	−0.020	−0.016	−0.016	−0.016

Due to very high gradients in the vicinity of points of vanishing slip segments, the accuracy of the method decreased, when passing those points during calculations. However, except for a small distance from those points, the method used in numerical simulation appeared to be accurate. Results obtained for different pairs of approximation parameters m and n were compared in the neighbourhood of the point of vanishing of slip segments and the difference between the two solutions is given in Table 4. Slip segments 4 and 5 disappear at load parameter $t = 2.41004$ for $m = 8$, $n = 6$, and at $t = 2.41011$ for $m = 12$, $n = 10$. The values of J_3^* and J_4^* are most sensitive at these states.

8.3. *Cyclic loading programs*

Vanishing of slip segments can also be observed in all cyclic loading cases. The symmetric cyclic response is presented in Fig. 10. After few loading cycles, a nearly asymptotic state is achieved. The symmetric and nearly steady hysteresis loop is observed just after one full cycle, Fig. 10b, while slip segment system shows nearly cyclic changes after three cycles, Fig. 10a. Then, when the number of cycles increases, it is seen, that while at each load reversal point new slip segments are created, 7th and 8th slip segments vanish at each cycle. Furthermore, only the first eight or nine segments can be called "active", while others only move very slowly apart from the tip.

The symmetric cyclic loading with two amplitudes is shown in Fig. 11. Two and a half cycles with amplitude $[-1,+1]$ are followed by cyclic loading with amplitude $[-0.5,+0.5]$. Then after few cycles the slip segment lengths change in a cyclical manner. Again only the first six slip segments are "active". The hysteresis loop is not symmetric, but it has a tendency to become symmetric, Fig. 11c. It seems, that also this loading case has its steady cyclic state, though it was not attained in the computation process.

Oppositely, in the non-symmetric cyclic loading case $[0,+1]$, no asymptotic state has been found, as shown in Fig. 12. After 20 cycles both the total slip zone length L^*, Fig. 12b, and the maximum tip rotation Θ^*_{max}, Fig. 12c, are still increasing. Three cases are possible here. First, that no steady state exists, second, that the number of transient cycles is finite, but very large so it cannot be computed due to constraints of the method, and thirdly the asymptotic state was not computed because of accumulated numerical errors. However, since there is no reason for numerical errors to be bigger then in other loading cases, the third explanation does not seem plausible. Similarly, when compared to symmetric loading cases, a very large number of transient cycles does not seem plausible. So it is possible that an interesting feature of the system has been found, namely that the non-symmetric loading response has no asymptotic state.

A very important fact can be observed in all loading cases, namely that all points O_i move apart from beam tip during loading process. In fact, it is seen in Figs 7–11, that all curves representing functions $J_i^*(t)$ are always monotonically increasing. As a result, the total length of the slip zone also is monotonically growing, which confirms our basic assumption (14). Furthermore, since the decreasing of any function $J_i^*(t)$ was not observed, their growth seems to be a rule, but having no explanation nor proof at the moment.

The model presented allows numerical calculation of a beam response for an arbitrary loading history. Semi-similar solutions in cases of proportional monotonic loading have been found. Unloading, reloading and cyclic loading programs have also been presented, showing interesting features of the system. Asymptotic transient states occur in two general cases: when the applied load is bigger than the maximum load value of previous load history (unloading and reloading), Figs 7–9, and in case of symmetric cyclic loading, Figs 10 and 11. Further, the same load–displacement characteristics can be obtained for the same steady cyclic loading, but for different slip segment layouts, resulting from different loading histories, Fig. 11.

9. CONCLUDING REMARKS

The present solution complements the previous treatments by Fischer *et al.* (1991) and Nikitin (1992), by accounting for an infinite number of slip zones propagating from the loaded beam tip and by allowing for non-monotonic loading. Interesting features of the system have been shown for both monotonic and cyclic loading. The solution is valid for a finite beam provided the length of slip zone is less than the beam length and there is no interaction with end boundary conditions. The problem of a finite beam and transition from the slip to slide mode will be treated separately.

The case of the beam loaded by the concentrated moment at its tip, which was extensively treated in numerical examples, is fully equivalent to the case of a beam deformed by a cross-sectional temperature gradient constant along the beam length, treated in Fischer *et al.* (1991). The results are in qualitative agreement with those of Fischer *et al.* (1991). Also, as it was discussed in Section 8.1, practically the same results as compared to Nikitin (1992) were obtained for monotonic loading of an infinite beam.

The incremental numerical method requires a considerable computing time, especially for cyclic loading programs. The incremental steps must be sufficiently small in order to describe slip segment evolution and their disappearance, moreover, minimization procedures must be applied at each time step.

The elastic friction model discussed in Section 6 provides an analytical solution which differs only by a maximum of 10% from the slip friction model in the case of monotonic loading. However, for cyclic loading the elastic friction model should be reformulated in

order to properly describe the forms of hysteresis loops. This problem was not discussed in the paper.

Acknowledgement—The present work was partially supported by the Science Research Council (KBN), Grant No. 3 1014 91 01.

REFERENCES

Duvaut, G. and Lions, J. L. (1973). *Les inequations en mecanique et en physique*. Dunot, Paris.

Fischer F. D., Hinteregger E. and Rammerstorfer F. G. (1991). A computational study of the residual stress distribution in thermally loaded beams of arbitrary cross-section on frictional support. *Nonlinear Computational Mechanics—State of the Art* (Edited by P. Wriggers and W. Wagner), pp. 737–750. Springer-Verlag, Berlin.

Fischer, F. D. and Rammerstorfer, F. G. (1991). The thermally loaded heavy beam on a rough surface. *Proc. 8th Symposium on Trends in Applications of Mathematics to Mechanics* (Edited by F. Ziegler), pp. 10–21. Longman Higher Education & Reference, Burnt Mill.

Jarzębowski, A. and Mróz, Z. (1994). On slip and memory rules in elastic, friction contact problems. *Acta Mechanica* **102,** 199–216.

Mróz, Z. and Jarzębowski, A. (1993). Phenomenological model of contact slip. *Acta Mechanica* **102,** 59–72.

Mróz, Z. and Stupkiewicz, S. (1994). An anisotropic friction and wear model. *Int. J. Solids Structures* **31,** 1113–1131.

Nikitin, L. W. (1992). Bending of a beam on a rough surface (in Russian). *Dokl. Ak. Nauk* **322,** 1057–1061. (See also English translation: *Sov. Phys. Dokl.* **37**(2), 98–100, 1992, American Inst. Physics.)

Zingone, G. (1968). Limit analysis of a beam in bending immersed in an elastoplastic medium. *Meccanica* **3**(1), 48–56.